# Uncertainty Quantification for Modern Antenna Systems

Oscar Borries, Erik Jørgensen, Min Zhou, Jakob Rosenkrantz de Lasson

TICRA, Copenhagen, Denmark
{ob,ej,mz,jrdl}@ticra.com

***Abstract*—Many modern antenna systems, particularly for applications in telecommunication or earth observation, have significant mechanical complexity. This entails an often lengthy and detailed design process, where the design is carefully revised to ensure the best performance for the intended application. In particular, the electrical design often needs to take into account uncertainties in the mechanical design. In this paper, we present an efficient way of quantifying the effects of uncertainties by using electromagnetic simulation of the antenna design with mechanical uncertainties added to the model of the antenna. The methods shown here far outperform the conventional Monte-Carlo techniques, both in terms of accuracy and computational time.**

## I. Introduction

Designing antenna systems for modern telecommunication or earth observation applications entails stringent performance requirements and strict error budgets. As the systems become increasingly complex and involve many subsystems, the need for accurate and reliable quantification of the imperfections involved in the error budgets becomes greater and greater. In particular, for concepts such as unfurlable reflectarrays or unfurlable reflectors, where in-flight deployment is used, detailed mechanical and thermal studies are required, all of which provide parameter ranges rather than specific parameter values.

Modern computational electromagnetics software makes it possible for the RF engineer to simulate a large number of the mechanical designs, and in some cases the software can allow fully automatic optimization to attain optimal performance. However, when it comes to quantifying the uncertainty, i.e., the performance degradation introduced by mechanical imperfections, the engineers are on their own.

If the engineers apply some form of uncertainty analysis, most will resort to simply running a very large number of simulations with random errors added sporadically to the system, and then perform some statistical examination on that data, a so-called *Monte-Carlo* simulation. The downsides to this approach are clear: A very large number of simulations is required, and the risk of user error is high. Further, as we will show later, the statistical accuracy is extremely poor, which could cause misleading conclusions about the final performance when the antenna is deployed.

This paper presents an alternative approach. The user is required to specify how the errors manifest themselves in the system, e.g. surface errors on the reflectors or an undesired reflector tilt, inaccurate mounting or phase errors in the feed, and so on. Based on this input, the algorithm automatically determines the uncertainty of the output parameter of interest, e.g. peak directivity, return loss or even full radiation patterns, with accuracy that far surpasses the simple Monte-Carlo approach.

The paper is structured as follows. After an introduction to Uncertainty Quantification (UQ) in Section II, including a demonstration of how these algorithms greatly outperform Monte-Carlo sampling, we present a number of test cases in Section III that illustrate how the method is able to quantify the performance uncertainty caused by geometrical errors in the design.

## II. Mathematical Uncertainty Quantification

Uncertainty Quanfication (UQ) has in the recent years seen a significant increase in interest within the applied mathematics community, particularly due to progress made in areas such as stochastic collocation.

The fundamental question that UQ attempts to answer is:

> Given a function $F(\overline{X})$, where $\overline{X}$ is a vector of $D$ stochastic elements, characterize the behaviour of $F(\overline{X})$.

How to characterize the behavour, however, is not straightforward. The traditional approach is the Monte-Carlo method, which simply samples the function $F$ a large number of times by picking $\overline{X}$ according to the distribution of its elements. Aside from being very simple to implement, the Monte-Carlo method has the advantage that its convergence rate is $\frac{1}{\sqrt{M}}$, where $M$ is the number of evaluations of $F$, and thus the convergence speed is independent of the number of parameters $D$ in the $\overline{X}$ vector.

The drawback, however, of Monte-Carlo is that in practice, $\frac{1}{\sqrt{M}}$ is simply far too slow for many applications, in particular scenarios where high accuracy is needed, where $F(\overline{X})$ is time-consuming to evaluate, and/or where the number of parameters $D$ is not large. This drawback can be understood by considering Monte-Carlo as a piece-wise constant approximation to the cumulative distribution function of $F(\overline{X})$.

To improve on the Monte-Carlo performance, methods based on higher-order approximation such as Stochastic Collocation (SC) or Polynomial Chaos Expansion (PCE) offer a far better convergence rate for a moderate number of parameters $D$, while only being slightly more complicated to implement.

Stochastic collocation is done by approximating the moments of the function $F$ by numerical integration:

$$\textbf{Expected value}: \quad \mathrm{E}(F(\overline{X})) = \mu_F \tag{1}$$
$$= \int_{a^{(1)}}^{b^{(1)}} \int_{a^{(2)}}^{b^{(2)}} \cdots \int_{a^{(D)}}^{b^{(D)}} g_X(\overline{X}) F(\overline{X}) d\overline{X},$$
$$\textbf{Variance}: \quad \mathrm{Var}(F(\overline{X})) = \sigma_F^2 \tag{2}$$
$$= \int_{a^{(1)}}^{b^{(1)}} \int_{a^{(2)}}^{b^{(2)}} \cdots \int_{a^{(D)}}^{b^{(D)}} g_X(\overline{X}) F^2(\overline{X}) d\overline{X} - \mu_F^2.$$

In this notation, $g_{X^{(i)}}$ is the distribution function for the $i$'th element in $X$, and $a^{(i)}$ and $b^{(i)}$ are the limits of this distribution function. The most common distributions are shown below:

| Distribution | $g_X(x)$ | $[a, b]$ |
|---|---|---|
| Normal | $\frac{1}{\sqrt{2\pi}} e^{\frac{-x^2}{2}}$ | $[-\infty, \infty]$ |
| Uniform | $\frac{1}{2}$ | $[-1, 1]$ |
| Exponential | $e^{-x}$ | $[0, \infty]$ |

Polynomial Chaos Expansion is done by approximating the behaviour of the function $F$ by orthogonal polynomials, chosen according to the Wiener-Askey scheme. The details are found in [1], [2], [3].

Regardless of whether stochastic collocation or polynomial chaos expansion is used, uncertainty quantification allows for a range of statistical estimates to be obtained:

- **Mean performance:** What is the expected (mean) performance of the system?
- **Variation in performance:** What is the variation in the performance of the system?
- **Deviation from nominal:** How does the expected performance deviate from the nominal performance?
- **Confidence intervals:** With $\alpha$-percent certainty, how will the system perform?

These estimates are often required when designing antennas for industrial applications. Further, if polynomial chaos expansion is used, the so-called Sobol indices can be computed, which can then answer the question

- **Partial variance:** How much of the variation in performance is caused by a specific variable?

This has a range of benefits in terms of cost-based reduction of uncertainty, see. e.g. [2]. For instance, if it turns out that a single variable is responsible for, say, $80\%$ of the variation in the performance, it is clear that it will be worthwhile increasing the reliability of that variable.

From a numerical standpoint, the difference in practice between the convergence rate of Monte-Carlo (MC) and higher-order methods (SC or PCE) is extreme for a moderate number of unknowns. We will demonstrate this with an example, inspired by [2].

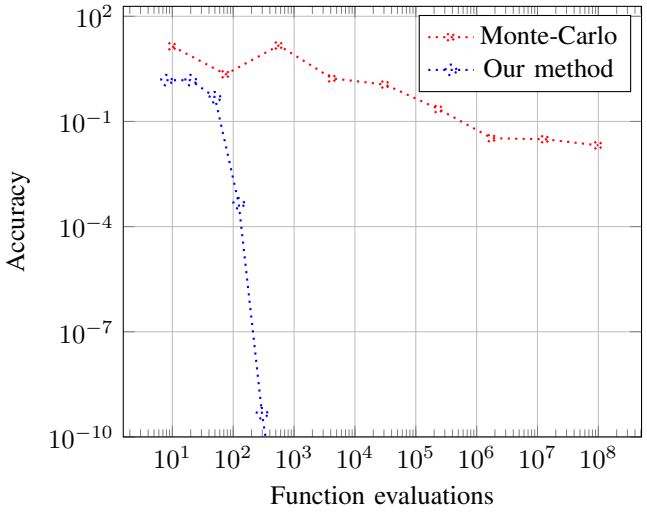


Fig. 1. A comparison of the convergence rate for Monte-Carlo and Stochastic Collocation when used to determine the mean of the stochastic Ishigami function (3).

Consider the so-called Ishigami function of the stochastic variables $x_1, x_2, x_3$:

$$f(\overline{x}) = \sin(x_1) + a\sin^2(x_2) + bx_3^4 \sin(x_1) \tag{3}$$

where $x_1, x_2, x_3$ are uniformly distributed between $[-\pi, \pi]$. The expected value and variance can be computed analytically based on (1) and (2), giving $\mu_f = a/2$ and $\sigma_f^2 = 1/2 + a^2/8 + b\pi^4/5 + b^2\pi^8/18$. Based on this, we can examine the number of function evaluations required for convergence of e.g. the mean, as shown in Figure 1, for $a = 3$ and $b = 5$.

The results clearly show the points raised above concerning the difference in performance between MC and higher-order UQ methods — MC converges extremely slowly, and requires several orders of magnitude more evaluations than Stochastic Collocation, even when considering only modest accuracy levels of about $10^{-2}$ relative error. If better accuracy than that is needed, which is particularly relevant when considering wide (e.g. $99\%$) confidence intervals, then Monte-Carlo is simply not a realistic option.

## III. Results

With these conclusions in mind, we will now look at three cases where we apply uncertainty quantification to antenna designs where manufacturing or deployment issues are important to take into account when designing the antenna. We note that all simulations are performed on a 2016 Macbook Pro laptop.

### A. Unfurlable Mesh Reflector

We consider an unfurlable mesh reflector at C-band. The specific configuration is shown in Figure 2, where a triangular mesh is shown with black lines. The nodes of the mesh sit exactly on the surface of the nominal parabolic reflector, and these nodes are connected by planar triangles. For the specific antenna, the offset nominal reflector has a projected aperture

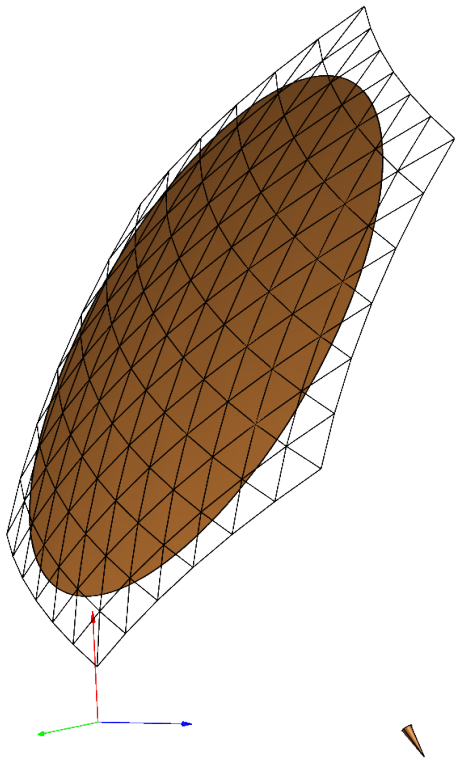

Fig. 2. An illustration of the meshed reflector analysed in Section III-A.

diameter of 4.7 m, a focal length of 3.3 m, and a clearance of 1.15 m; the frequency is 6.9 GHz. For the mesh reflector, we consider a uniform hexagonal mesh with triangle side length of 0.5 m [4].

Unfurlable antennas present a range of mechanical issues in order to achieve satisfactory and indeed reliable performance, and thus represent a relevant showcase for the potential of higher-order UQ techniques in antenna design.

We begin by varying the mounting angles of the reflector, imagining a scenario where the unfolding of the reflector relative to the feed has, in some way, produced an angular distortion of the reflector. At the bottom of Figure 2, the coordinate system indicates the imagined anchor point of the reflector, and we rotate the reflector both around the blue axis and the green axis, letting those two angles be uniformly distributed between $\pm 0.1°$.

The uncertainty quantification algorithm runs in about a minute on a laptop, with each seperate analysis of the configuration analysed using TICRAs software GRASP, applying Physical Optics augmented by the Physical Theory of Diffraction. The result is shown in Figure 3 which shows the co-polar component in the $\phi = 0$ plane. We notice quite large confidence intervals, indicating that the performance is quite sensitive to the uncertainty in mounting angles. This is particularly pronounced for the innermost sidelobes, while the interval is smaller for the grating lobe [4] that is seen around $\theta = -10°$.

We then move to consider uncertainty in the mesh nodes of

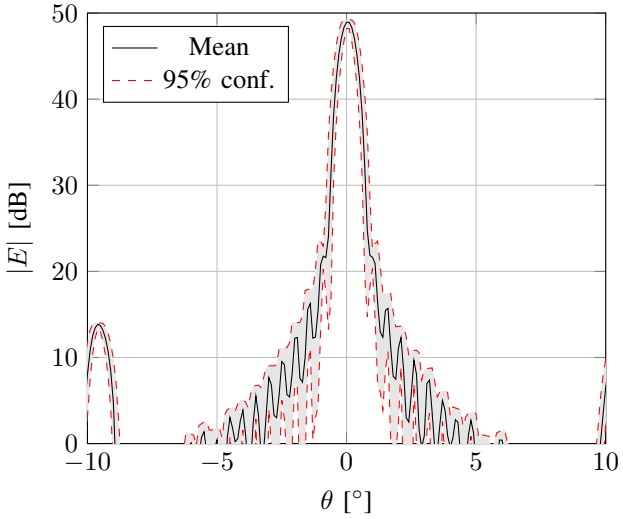


Fig. 3. Effects on the co-polar pattern in the $\phi = 0$ plane as uncertainty is introduced to the mounting angles.

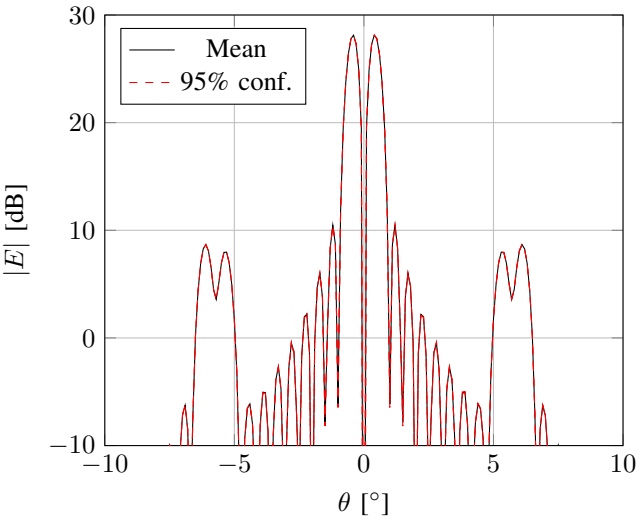


Fig. 4. Effects on the cx-polar pattern in the $\phi = 90°$ plane as uncertainty is introduced to the mesh surface nodes.

the triangular, considering a scenario where each of the 127 nodes are displaced independently in $z$, with a $\pm 30$ micron uniformly distributed uncertainty. Now, the analysis requires 3:30 minutes and the result is shown in Figure 4, where we consider the cx-polar component in the $\phi = 90°$ plane. The variation of the cx-polar component for the considered uncertainty in the mesh surface nodes is extremely small, revealing a robustness of the antenna performance to the exact node positions.

### *B. Reflectarray*

We then move to consider a reflectarray discussed in the literature [5], a planar array with specifications as described in Table I. The reflectarray elements are optimized to provide a high gain over a European coverage, as illustrated by Fig. 5.

TABLE I
REFLECTARRAY DATA

| | |
|---|---|
| Center frequency | 10 GHz |
| Frequency range | $9-11$ GHz |
| Number of elements | $50 \times 50$ |
| Reflectarray dimensions | 600 mm $\times$ 600 mm |
| Relative permittivity | $\epsilon_r = 3.66$ |
| Substrate thickness | $d = 1.524$ mm |
| Loss tangent | $\tan\delta = 0.0037$ |

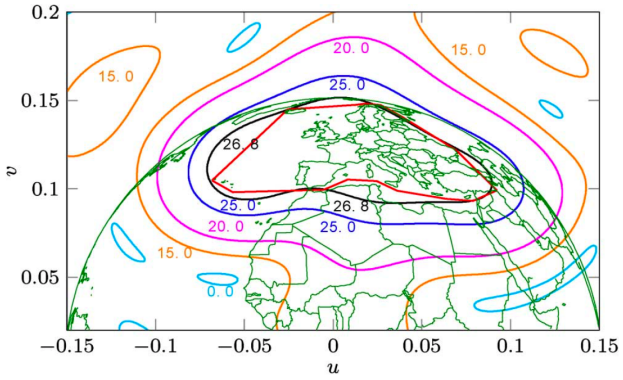


Fig. 5. Co-polar radiation pattern of the reflectarray specified in Table I.

We consider the effect of adding an uncertainty to the size of the square elements, such that a small deviation from the optimized sizes are added, uniformly distributed in the range $\pm 0.03$ mm, resulting in $D = 2500$ variables. We then consider the resulting uncertainty in the co-polar and cx-polar levels, applying the UQ algorithm requiring 7501 evaluations to converge. Due to the fast analysis algorithm [5], the entire UQ task requires less than two hours of computation time on a laptop.

The resulting 95% confidence interval for the minimum directivity in the coverage is $27.3 \pm 0.02$ dB. For most applications, this would be a very low sensitivity of the directivity to small uncertainties in the manufacturing. This result allows us to conclude that errors in the manufacturing of the elements will not significantly impact the performance of the array.

We then consider uncertainty of the relative permittivity of the dielectric substrate, for $\epsilon_r$ distributed as $U(3.56, 3.76)$, which means only a single variable and thus only a few simulations are necessary to produce the uncertainty quantification, requiring less than a minute of simulation time. The resulting uncertainty is shown in Fig. 6, demonstrating that the value of the relative permittivity significantly impacts the resulting pattern.

### C. Full reflector antenna system

As the final case, we consider a full reflector antenna system including feeding network, horn and reflector antenna, illustrating how the UQ algorithm can be used together with an advanced Generalized Scattering Matrix [6] framework to efficiently characterize the performance for the entire system as a function of changes in a subsystem.

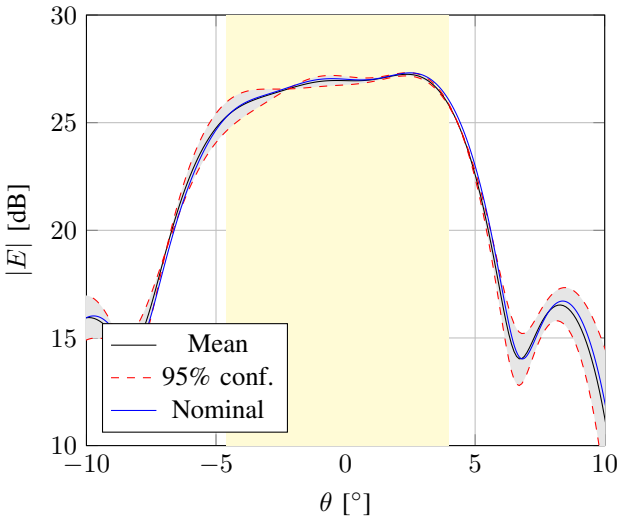


Fig. 6. Mean, 95% confidence interval and nominal ($\epsilon_d = 3.66$) pattern for the reflectarray when the relative permittivity $\epsilon_d$ of the dielectric substrate is uniformly distributed $U(3.56, 3.76)$. The performance of the reflectarray is clearly sensitive to $\epsilon_d$. Marked in yellow is the coverage area (the red zone in Fig. 5.

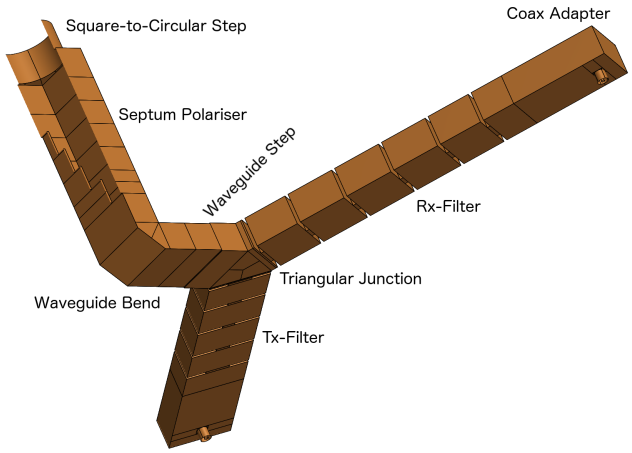


Fig. 7. Half of the feed network, with the other half obtained by mirroring along the open portion of the polariser and square-to-circular transition. Taken from [6].

The system is a feed chain and reflector assembly, intended for use as a Ku-band VSAT terminal. The reflector is a 1 m diameter rotationally symmetric antenna operating at $12.5 - 12.75$ GHz for Rx and $14.0 - 14.25$ GHz for Tx. The feeding network is illustrated in Figure 7, showing one of the diplexers with coax ports in a split view. The network produces RHCP in Tx and LHCP in Rx, with filters employed to improve the isolation. An illustration of the entire antenna is shown in Figure 8.

We add uniformly distributed variations of $\pm 0.5$ mm to step heights in the septum polariser shown at the top left side of Figure 7, and compute the effects on the peak directivity

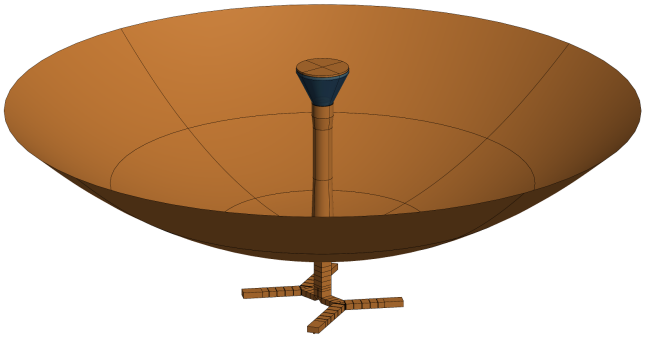

Fig. 8. The complete antenna, with the full feed network shown at the bottom, for the case in Section III-C. Taken from [6].

of the entire system at Rx. This requires about 20 minutes of computation time, providing a $95\%$ confidence interval of [39.38,39.42] dBi.

## IV. Conclusion

With state-of-the-art computational electromagnetics solvers, engineers are able to design increasingly complex high-performance antenna systems. However, when such systems are produced, the deviations from the computational model will result in performance degradation that the engineer should have taken into account earlier. When augmented with the UQ algorithms outlined above, which far surpass the performance of simple Monte-Carlo implementations, computational electromagnetics solvers will be able to guide engineers to produce antennas that will perform as good in practice as they did on the computer.

## Acknowledgment

The authors would like to thank Professor Jan Hesthaven from Ecole Polytechnique Fédérale de Lausanne for inspiration and guidance.

## References

[1] L. Ng and M. S. Eldred, "Multifidelity uncertainty quantification using nonintrusive polynomial chaos and stochastic collocation," in *AIAA/ASME/ASCE/AHS/ASC Structures, Structural Dynamics and Materials Conference*, 2012.

[2] T. Crestaux, O. Le Maître, and J.-M. Martinez, "Polynomial chaos expansion for sensitivity analysis," *Reliability Engineering & System Safety*, vol. 94, no. 7, pp. 1161–1172, Jul. 2009.

[3] A. C. M. Austin, N. Sood, J. Siu, and C. D. Sarris, "Application of Polynomial Chaos to Quantify Uncertainty in Deterministic Channel Models," *IEEE Transactions on Antennas and Propagation*, vol. 61, no. 11, pp. 5754–5761, Oct. 2013.

[4] J. R. de Lasson, C. Cappellin, R. Jørgensen, L. Datashvili, and J.-C. Angevain, "Advanced techniques for grating lobe reduction for large deployable mesh reflector antennas," in *IEEE Antennas and Propagation Symposium*, 2017.

[5] M. Zhou, S. B. Sørensen, O. S. Kim, E. Jørgensen, P. Meincke, and O. Breinbjerg, "Direct Optimization of Printed Reflectarrays for Contoured Beam Satellite Antenna Applications," *IEEE Transactions on Antennas and Propagation*, vol. 61, no. 4, pp. 1995–2004, 2013.

[6] N. Vesterdal, E. Jørgensen, P. Meincke, M. Simeoni, and B. Fiorelli, "Combined Optimisation of Reflector and Feed Systems ," in *38th ESA Antenna Workshop*, Noordwijk, The Netherlands, Oct. 2017.